6 W bias supply

Using the new 800 V CoolMOS™ P7, ICE5QSAG QR flyback controller, and snubberless flyback for improved auxiliary power-supply efficiency and form factor

Order code: **KIT_6W_12V_ICE5**

Author: Jared Huntington

Scope and purpose

In power supplies that are used for server, telecom and industrial applications there is typically a small bias power supply in addition to the main power converter. This bias supply is used to power the fan, controllers and any additional monitoring and control logic on the board. This application note gives an overview of a bias supply designed for the Infineon high-power demo boards. This bias board is designed to run in a system where it is continuously powered from the 400 V DC output of a boost Power Factor Correction (PFC) converter. This board uses the ICE5QSAG Quasi Resonant (QR) flyback controller and an 800 V CoolMOS™ P7 IPU80R4K5P7, which are the latest generation of devices. This design was done as a snubberless flyback converter to further improve the efficiency. These new Infineon devices and the snubberless operation give a 10.4 percent efficiency improvement with a 6 W load and a 25 percent improvement with a 1 W load compared to the previous bias board. The form factor was also improved to increase the system-level power density. This document contains an overview of the design decisions, an overview of the snubberless operation, performance benchmarking and guidance on how to adapt the board for other applications.

Intended audience

Power-supply design engineers

Table of contents

1 Overview and key results

In high-power supplies that are used for server, telecom and industrial applications, there is typically a small bias power supply in addition to the main power converter. This small bias supply powers the gate drivers, controllers, fans and any additional small-signal devices on the PCB. This controls the power-up sequence of the different sections of the power supply. A separate bias supply also ensures that monitoring and control circuitry will continue to run through fault conditions on the main supply. This bias power supply begins to play a larger role in the system losses at light load and under standby conditions.

This 6 W bias board was designed as a replacement for an existing bias board used in high-power Infineon demo boards. The goal was to be pin-to-pin compatible with the previous bias supply design, but to also to improve the efficiency and form factor, allowing for higher system-level power density. The previous bias board used the CoolMOS™ C3 technology, and this provided an opportunity to update the board with the latest Infineon devices.

The board has a 12 V output that is regulated on the primary side, and the secondary is an unregulated 12 V output. It is designed to provide 6 W of operation from 120 V DC to 440 V DC.

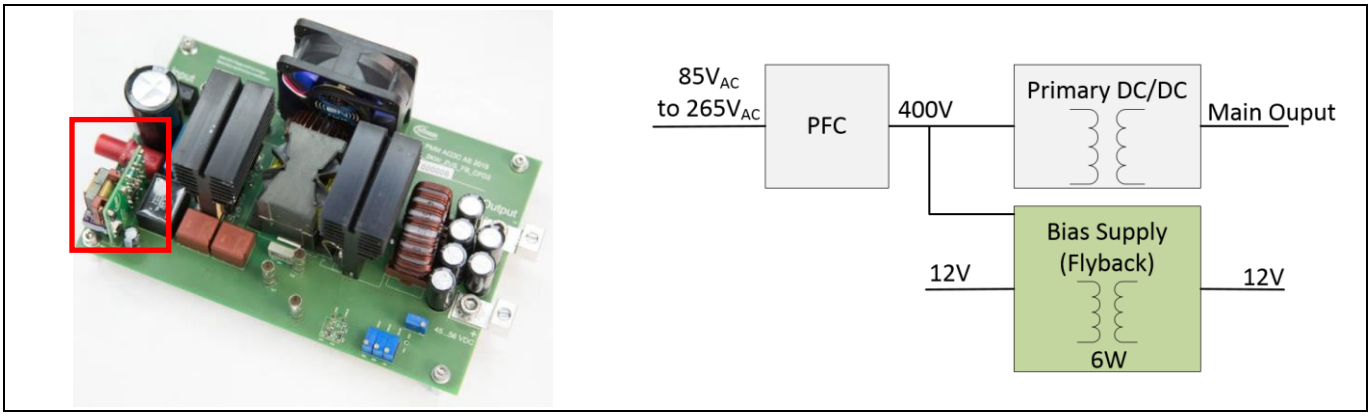

Figure 1 The picture on the left shows a 6 W bias board used in the Infineon 2 kW ZVS full-bridge demo board, and the block diagram on the right shows a typical configuration

The efficiency improvement of the new design can be seen below. The efficiency improvement is between 10.4 percent and 25 percent over the 1 W to 6 W load range. Below, the new bias board can be seen along with the reduction in the overall form factor.

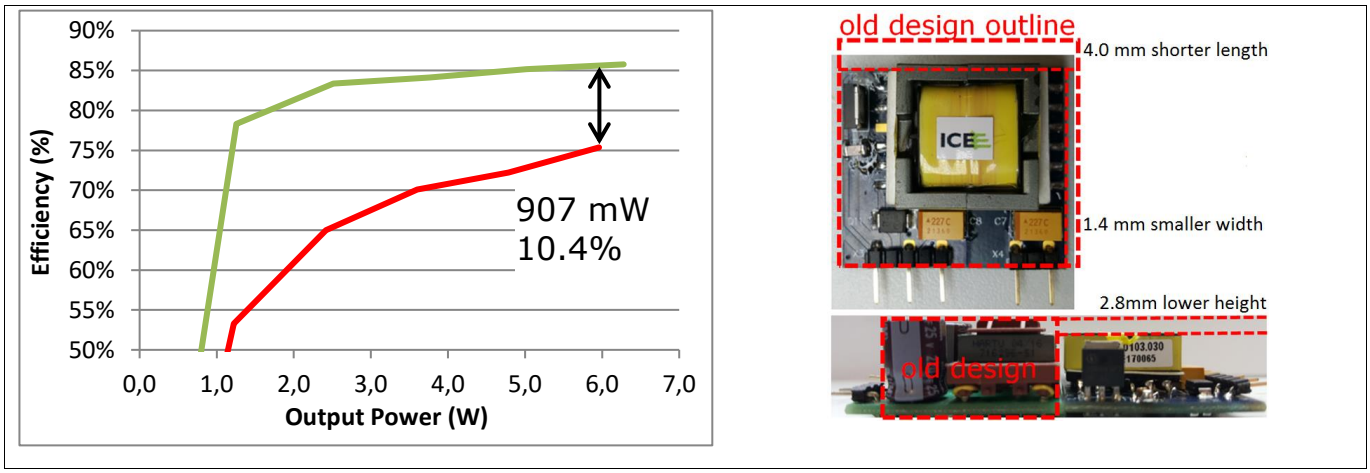

Figure 2 Improvement in efficiency at 400 V AC, and the form factor compared to the previous design

2 Design changes overview

2.1 Transitioning from CoolMOS™ C3 to 800 V CoolMOS™ P7

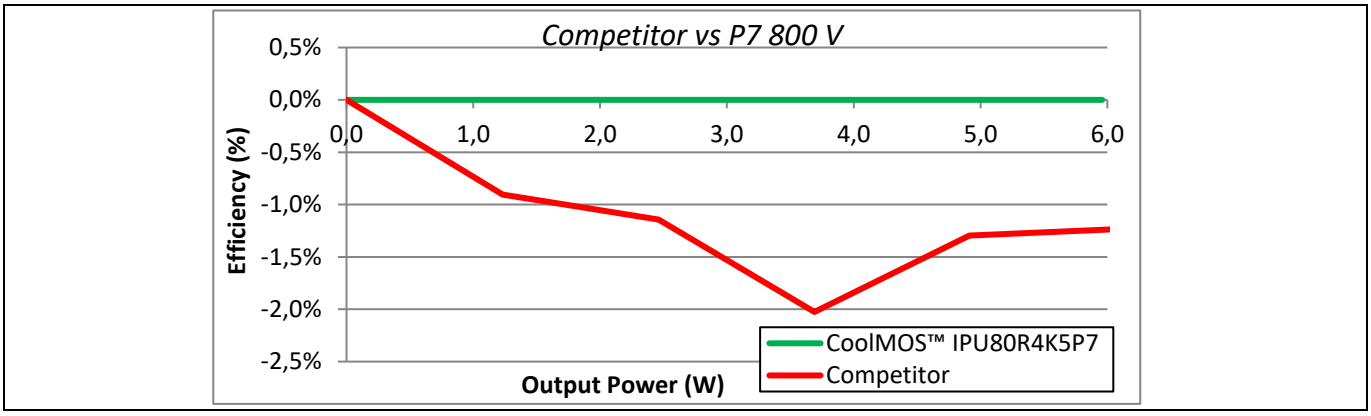

Figure 3 CoolMOS™ P7 compared to the closest-performing competitor in the 6 W bias board

The original bias board used the third-generation CoolSET™, which uses the C3 MOSFET technology. However, switching to the latest CoolMOS™ P7 offers better performance. The gate-driving losses of the device are lower, and the $R_{DS(on)}$ change vs temperature is lower than in the previous generation of devices. The P7 also has lower output capacitance energy storage vs voltage, but in this design some of these benefits are reduced by the additional C_{DS} capacitor that needs to be added for snubberless operation, as stated below. The efficiency compared to the closest equivalent competitor part is shown in Figure 3.

2.2 ICE5QSAG – QR flyback controller

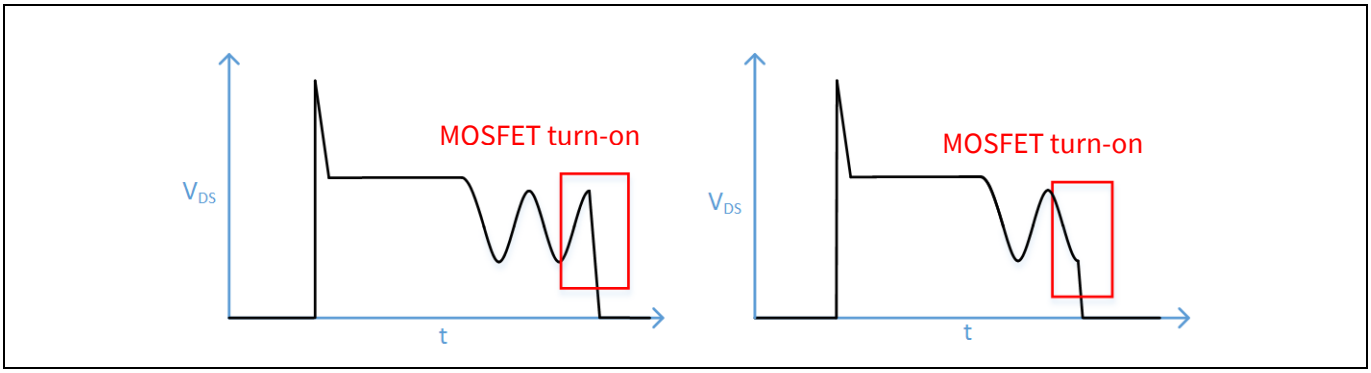

Figure 4 FF flyback primary MOSFET drain source waveform (left) vs a QR flyback primary MOSFET drain source waveform (right)

The design was switched from a Fixed Frequency (FF) flyback controller to the new ICE5QSAG standalone QR flyback controller. The QR flyback helps to reduce the switching losses in the MOSFET by using the Discontinuous Conduction Mode (DCM) resonant period of the flyback, and then only turning on the MOSFET in this valley.

Since the turn-on switching losses are a function of V^2 (as shown below), this reduces the overall system switching losses. This has the added benefit of lowering the amount of switched energy, which helps reduce switching noise from the converter, resulting in lower radiated and conducted emissions.

$$P_{sw\_on} = 0.5 f_{sw} C_{OSS} V_{DS}^2$$

2.3 Snubber network

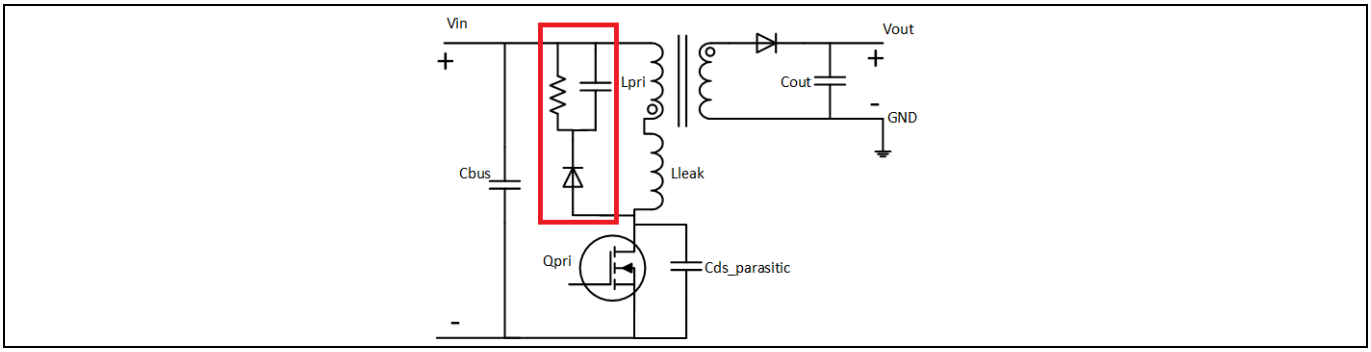

Figure 5 The image shows the typical RCD snubber network. In this design the snubber was removed to increase efficiency.

The original bias board design used an RCD snubber network. This network dissipates energy every switching cycle regardless of the load, since the RCD capacitor is charged to the reflected voltage of the secondary. By removing the snubber network and switching to a snubberless design, the overall efficiency was improved. This was done using a MOSFET with an 800 V breakdown voltage, which also helps with the margin in snubberless operation. 10 percent margin was kept from the drain source breakdown voltage to the peak drain source voltage seen on the MOSFET during full load and maximum DC input voltage operation. An overview of the snubberless concept will be provided in the next section of the application note.

2.4 Transformer

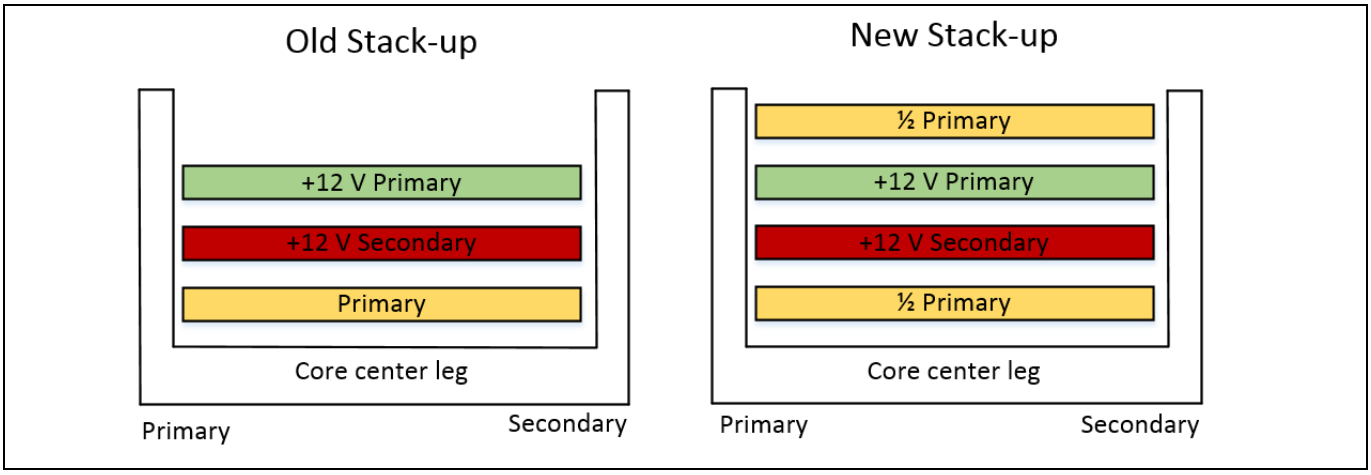

Figure 6 The single-layer construction is shown on the left, while the right-hand diagram shows the new interleaved transformer construction with a split primary winding to lower the leakage inductance

The transformer design was changed from a single stacked design to an interleaved design. This can be seen in Figure 6 (on the right) where the primary is split in half and stacked on the top and the bottom of the transformer stack-up. This helps to reduce the leakage inductance from the primary to the secondary, which affects the regulation of the secondary voltage because this is an unregulated winding. Reducing the leakage inductance is critical for the snubberless design of the system, because this additional leakage energy needs to be transferred to the total C_{DS} capacitance. This ends up determining what C_{DS} external ceramic capacitance is required, which has an overall effect on the system efficiency.

2.5 Output capacitors

Figure 7 Output capacitors were changed to tantalum polymer capacitors for higher density

The capacitors were changed from 25 V electrolytic capacitors to 16 V tantalum polymer capacitors to reduce size. Because tantalum capacitors are a reliability concern when their rated voltage is exceeded, a 14 V Zener was also added to the unregulated secondary rail to ensure that the secondary never goes beyond 14.5 V, even with the primary fully loaded and the secondary unloaded.

3 Snubberless flyback design

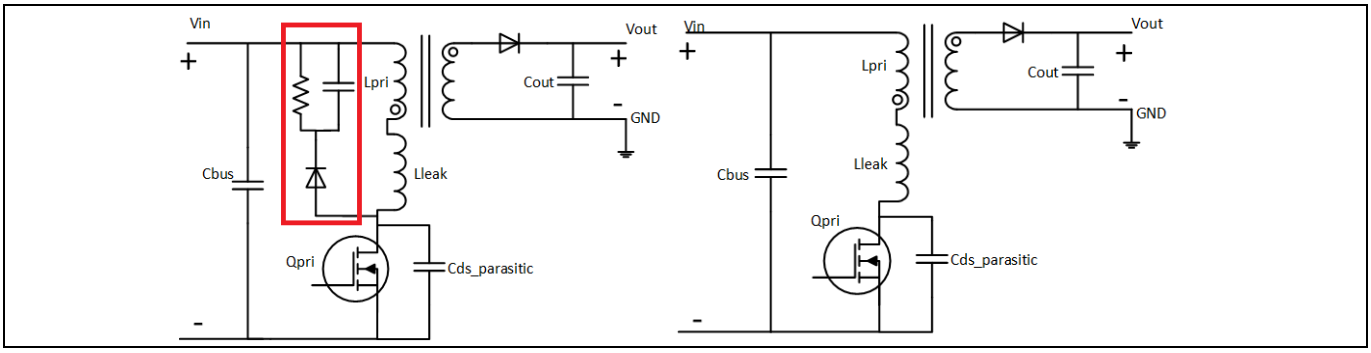

Figure 8 The typical RCD snubber configuration is shown on the left. The snubberless configuration where this RCD network is removed is shown on the right.

The original bias board design was done using an RCD snubber network. By removing the snubber network and switching to a snubberless design, the bias efficiency was improved. Switching losses and snubber losses play a significant role in the losses of this supply due to the high voltage operation, with a 380 V DC nominal input voltage and the fact that this is a low-power flyback in which system conduction losses are minimal. In addition to improving the system efficiency, the snubberless flyback converter also reduces the necessary PCB area and removes the cost of the RCD network.

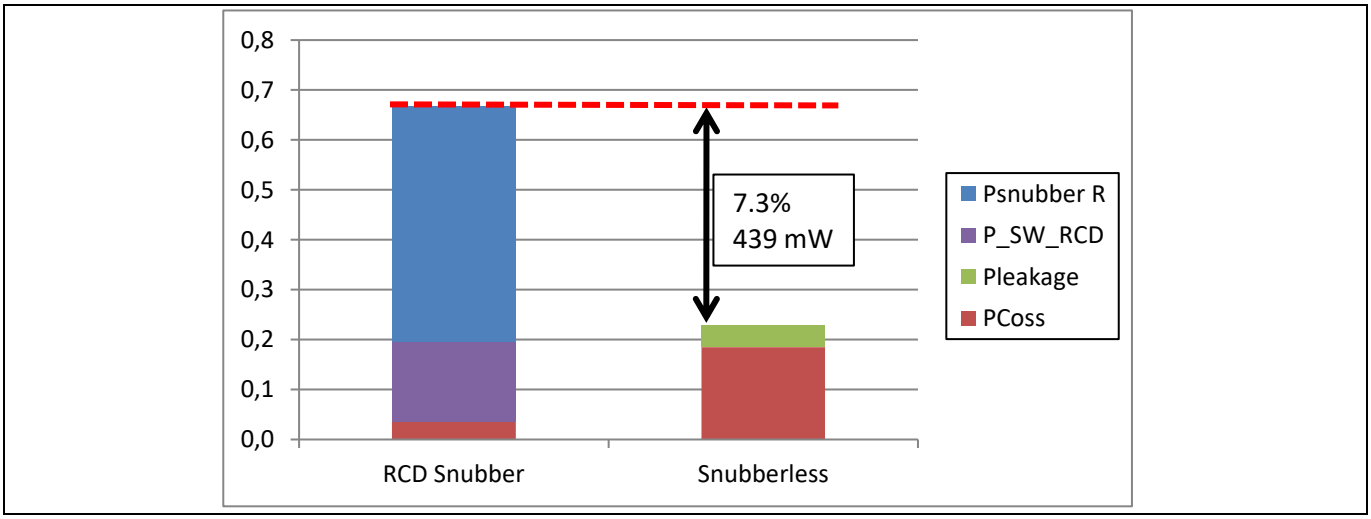

Figure 9 Transitioning to a snubberless flyback reduces power losses by 439 mW (7.3%)

The losses of the system are reduced in a snubberless design due to the removal of two key loss mechanisms. The first is that the RCD network charges to the reflected voltage every switching cycle, regardless of the system load. The leakage inductance energy also increases this voltage leading to further losses across the snubber resistor. The second loss mechanism comes from the additional capacitance added to the switching node from the RCD network, as well as the need to charge the capacitance across the RCD diode junction. These loss mechanisms are eliminated by the removal of the RCD snubber network.

To keep the MOSFET drain source voltage from becoming too high, an additional drain source capacitance is added across the drain node of the MOSFET. This leads to a higher C_{DS} switching loss when compared to the design with a snubber network, as shown in Figure 9 in red. The energy stored in the transformer leakage inductance gets dissipated in the high frequency copper loss of the transformer rather than in the RCD network. The calculated efficiency improvement in this design from removing the snubber is 439 mW, or around 7.3 percent at full load. These snubber losses are reduced throughout the output load range.

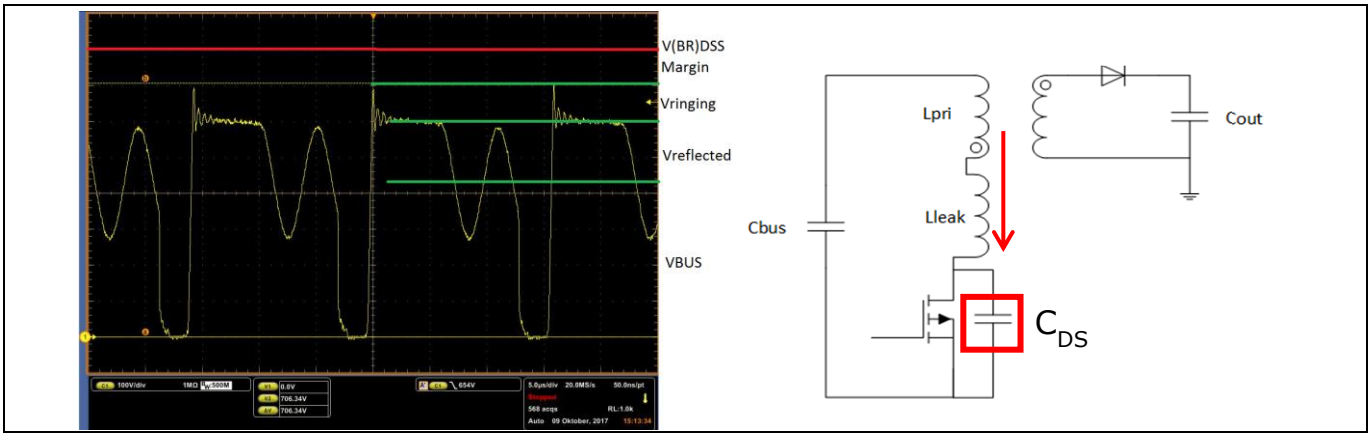

Figure 10 The MOSFET V_{DS} margin needs consideration for snubberless operation

In designing a snubberless flyback converter, it is critical to make sure the $V_{(BR)DSS}$ of the MOSFET is not exceeded. The V_{DS} of a MOSFET consists of three main sections, as shown in Figure 10. The V_{DS} is the total of the bus voltage (V_{bus}), the reflected voltage ($V_{reflected}$) and the ringing voltage ($V_{ringing}$). The ringing voltage of the MOSFET is the only portion that is affected in the transition from an RCD snubber to a snubberless design. To understand how to remove the snubber, the mechanism behind the drain source ringing needs to be understood.

When the MOSFET is turned on in a flyback converter, the current through the primary side of the transformer begins to ramp. When the MOSFET turns off, this energy then transfers to the secondary of the flyback converter. Not all of this energy transfers to the secondary, and the leakage inductance is the energy that cannot couple to the secondary. This energy then transfers to the total output capacitance of the MOSFET, which consists of the MOSFET C_{DS}, transformer parasitic capacitance, trace capacitance and any other capacitance on the drain node. An LC ringing occurs with the period set by the C_{DS} total and the $L_{leakage}$. To control the peak voltage of the drain source ringing, an external capacitance can be added in parallel to the drain source of the MOSFET. In this bias converter, an additional 100 pF capacitor on the drain source of the MOSFET was required to provide energy storage for the leakage energy at full load. A MOSFET with an 800 V breakdown voltage was used, which helps with the snubberless operation with a high voltage DC input. The peak drain source voltage at the maximum input voltage and maximum load was 706 V, which still gives 11.7 percent margin. A minimum of 10 percent margin should be kept from the drain source breakdown voltage.

Some equations to get a first estimate of the peak V_{DS} voltage are shown below. The voltage derived from these equations is then shown, to give the first estimate of the $V_{DS\ peak}$ compared to the measured value.

In this design the board is powered by the PFC, so 440 V would be the maximum input voltage, but the equation below would be used for a standard rectified universal-input (90 V AC to 265 V AC) flyback converter.

$$V_{bus} = V_{ACinput\_max}\sqrt{2} = 440\ \text{V}$$

The reflected voltage is the transformer turns ratio multiplied by the output voltage.

$$V_{reflected} = (V_{out} + V_{rectifier})\frac{N_{pri}}{N_{sec}} = 156\ \text{V}$$

The peak voltage caused by the ringing of the C_{DS} and leakage inductance can be approximated with all of the leakage energy transferring into the C_{DS} total capacitance.

$$V_{ringing} = I_{pk}\sqrt{\frac{L_{leakage}}{C_{DS\,total}}} = 119\ \text{V}$$

Adding these three voltage portions of the drain source waveform yields the peak drain source voltage.

$V_{DS\,peak} = V_{bus} + V_{reflected} + V_{ringing} = 715$ V, which is close to the measured 706 V $V_{DS\ peak}$.

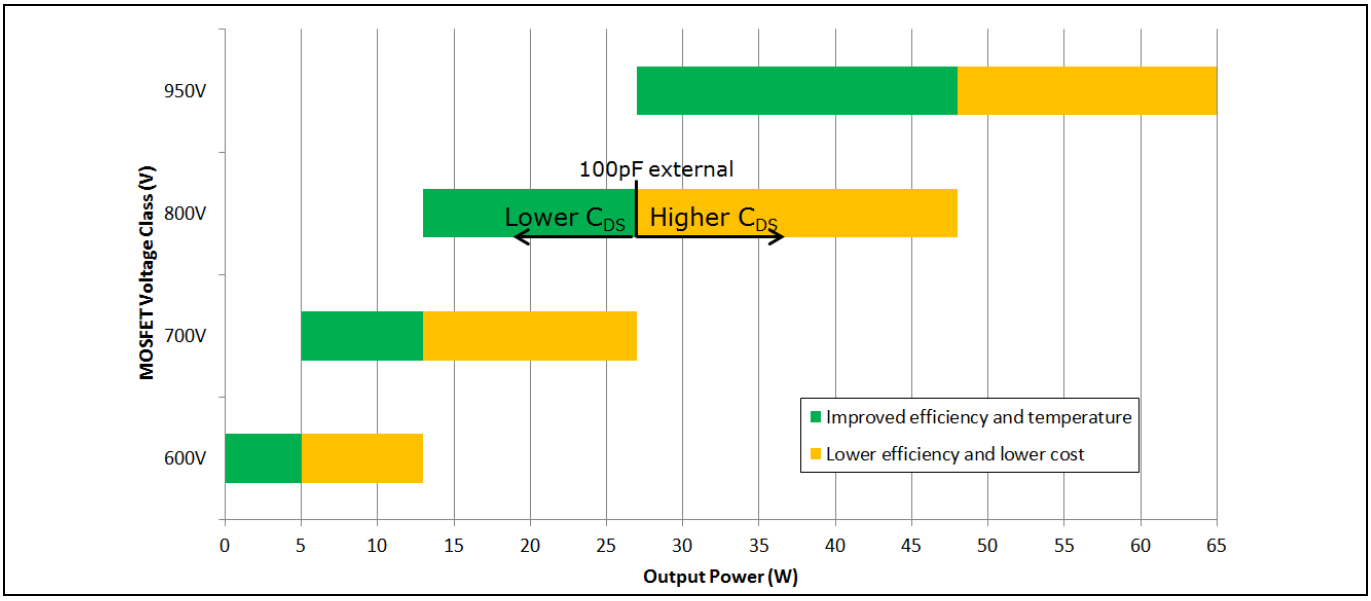

Figure 11 Snubberless flyback output power vs MOSFET voltage class for standard universal-input 90 V AC–265 V AC off-line power supplies

Looking at the benefits of the snubberless flyback operation, the question arises of where the snubberless concept is applicable. In a flyback converter the peak current on the input of the transformer increases as the system output power increases. Below is the equation for the peak current in a DCM flyback converter:

$$I_{pk} = \frac{2P_{in}}{V_{DCmin}D_{max}}$$

Looking at this peak current equation, it is clear that as the peak current increases with everything else held constant, the ringing and the $V_{DS\,peak}$ will also increase.

$$V_{ringing} = I_{pk}\sqrt{\frac{L_{leakage}}{C_{DS\,total}}}$$

This leads to the chart shown above, which takes common charger adapter DCM flyback requirements and looks at the $V_{(DS)BRR}$ voltage required for different output powers. This shows that as the output power of the system increases, a larger MOSFET breakdown voltage is required. This becomes a limiting factor in where a snubberless design can be used. Figure 11 does not match with this bias supply because the bias converter needs to run off 440 V DC maximum rather than the standard 375 V DC that would be common in a universal-input AC/DC supply.

The other aspect shown in this chart is that a snubberless flyback converter can be designed with a larger and larger C_{DS} to absorb the transformer leakage energy. There is a point where the required additional C_{DS} capacitance losses will match the R_{CD} snubber losses, and then the only benefit of the snubberless operation is reduced PCB area and system cost. This boundary is shown above by the transition from green to yellow.

From the graph above, it can be seen that for an efficiency benefit in snubberless operation, devices with a 600 V breakdown should be used below 5 W, the 700 V devices should be used to 13 W, 800 V devices can be used to 27 W, and 950 V devices can be used to 48 W. Going beyond these boundaries would reduce the system efficiency. The above graph makes several assumptions about the system design operating point, so these should be taken as guidelines rather than a hard boundary.

4 Possible design changes

4.1 Lowering the cost

The major cost center is the tantalum capacitors that were used to shrink the form factor. If cost is a priority, these capacitors can be replaced with 220 µF 16 V electrolytic capacitors to reduce the overall system cost at the expense of space.

4.2 Possible simplification

The discrete MOSFET could also be replaced with a CoolSET™ integrated controller, which combines the MOSFET and the controller in a single package. The MOSFET was left discrete to allow for further flexibility of testing different Infineon devices in different $R_{DS(on)}$ values and voltage classes. A part like ICE5QR4780AZ would have the equivalent CoolMOS™ device integrated.

5 Demo board overview

5.1 Demo board pictures

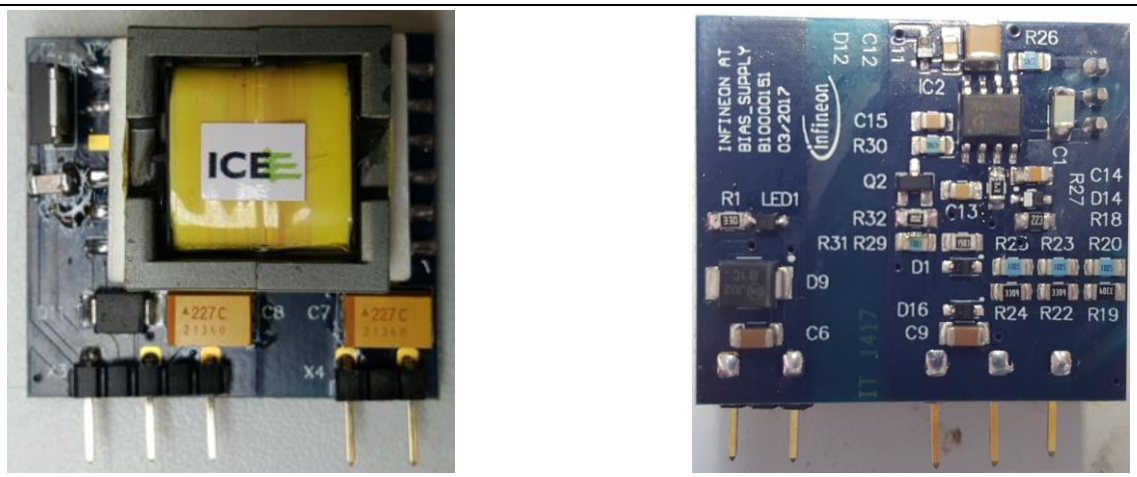

Figure 12 Top and bottom side of the 6 W bias board

5.2 Demo board specifications

Table 1

Section	Parameter	Specification
Input ratings	Input voltage	120 V DC to 440 V DC
	Peak efficiency 380 V AC, 6 W	85.8%
Output ratings	Nominal output voltage	12.0 V
	Output current	0.5 A
	Switching frequency	25 kHz to 60 kHz
Mechanical	Dimensions	Length: 31.2 mm Width: 35.1 mm Height: 14.7 mm Volume: 16.08 cm^3
Environmental	Ambient operating temperature	-25 °C to 50 °C

5.3 Schematic

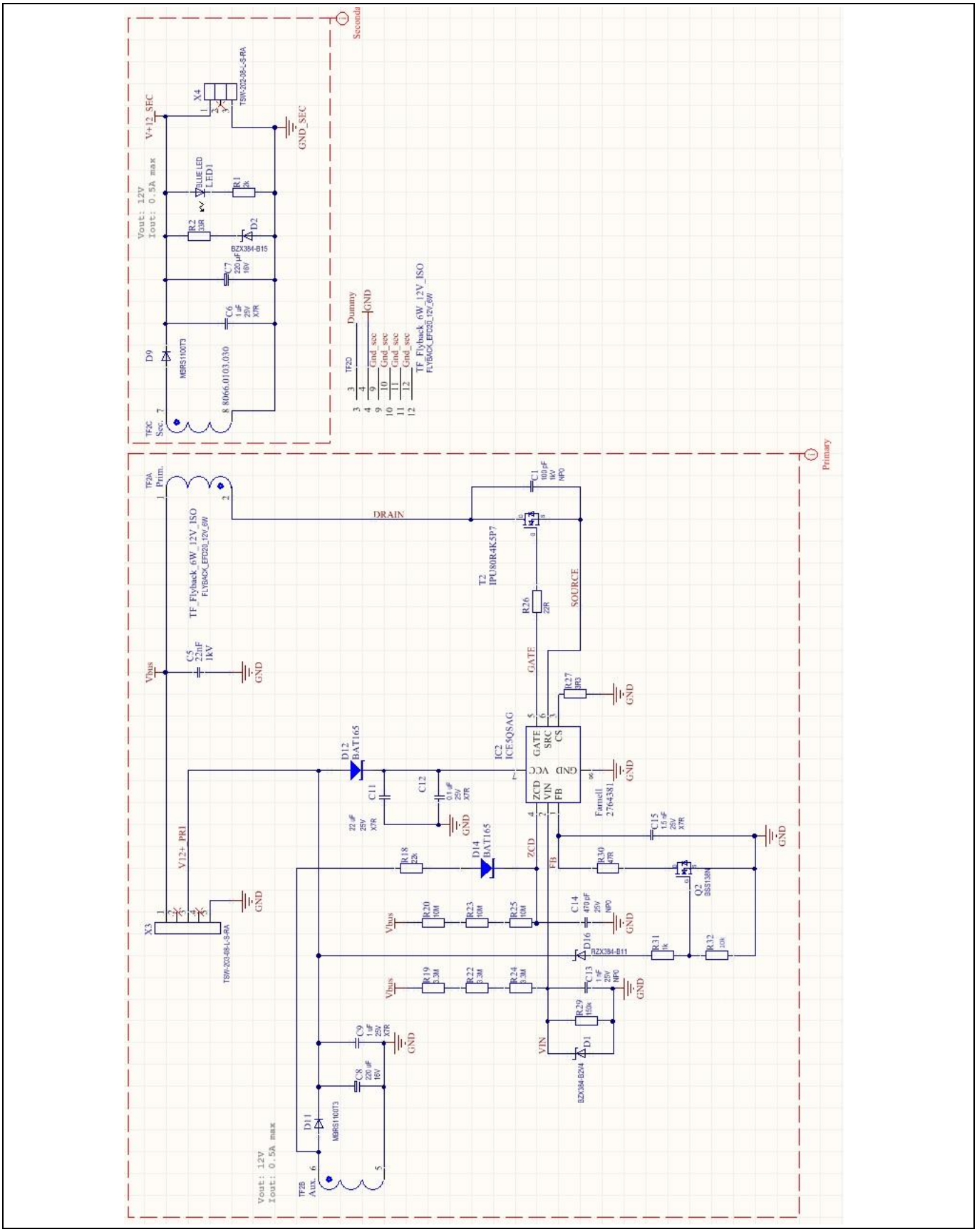

Figure 13 6 W bias schematic (details on BOM – register your board)

5.4 PCB layout

The PCB was designed using Altium Designer 16. Schematic and board files are available on request.

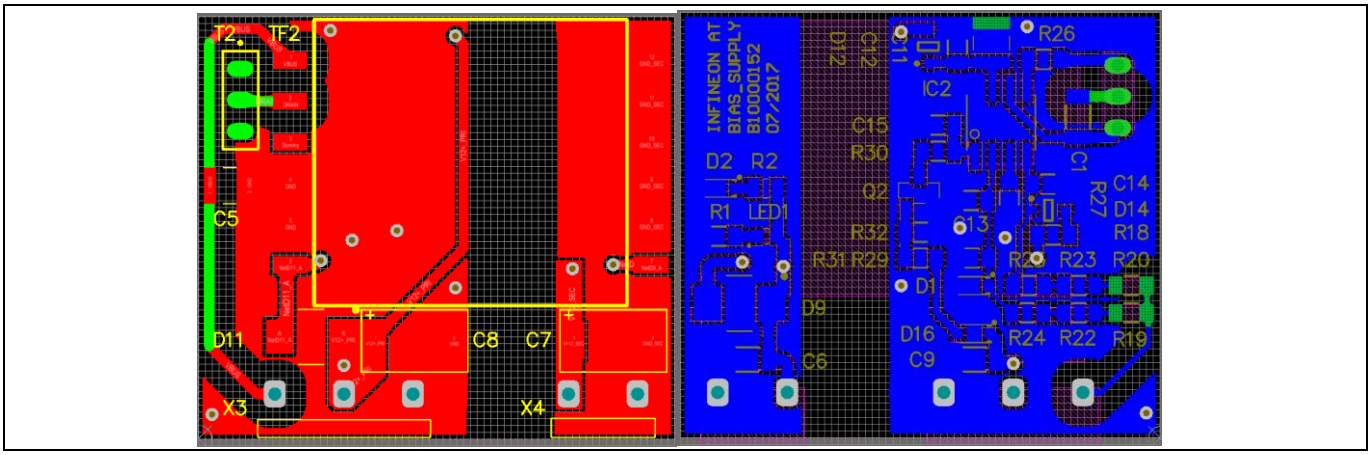

Figure 14 Board layout top and bottom

5.5 Transformer construction

The transformer was built by I.C.E. Transformers: http://www.icetransformers.com/

Table 2 Transformer specification

Manufacturer	I.C.E. Transformers
Core size	EFD20
Core material	3C95 or approved equivalent
Bobbin	Pin shine EFD20 SMT S-2005
Primary inductance	5000 µH measured from pin 1 to pin 2 @10 kHz
Leakage inductance	< 50 µH measured from pin 1 to pin 2 @10 kHz pins 5, 6, 7, 8 shorted

*100% of components are hipot tested to 4.2 kV primary to secondary for 1 minute.

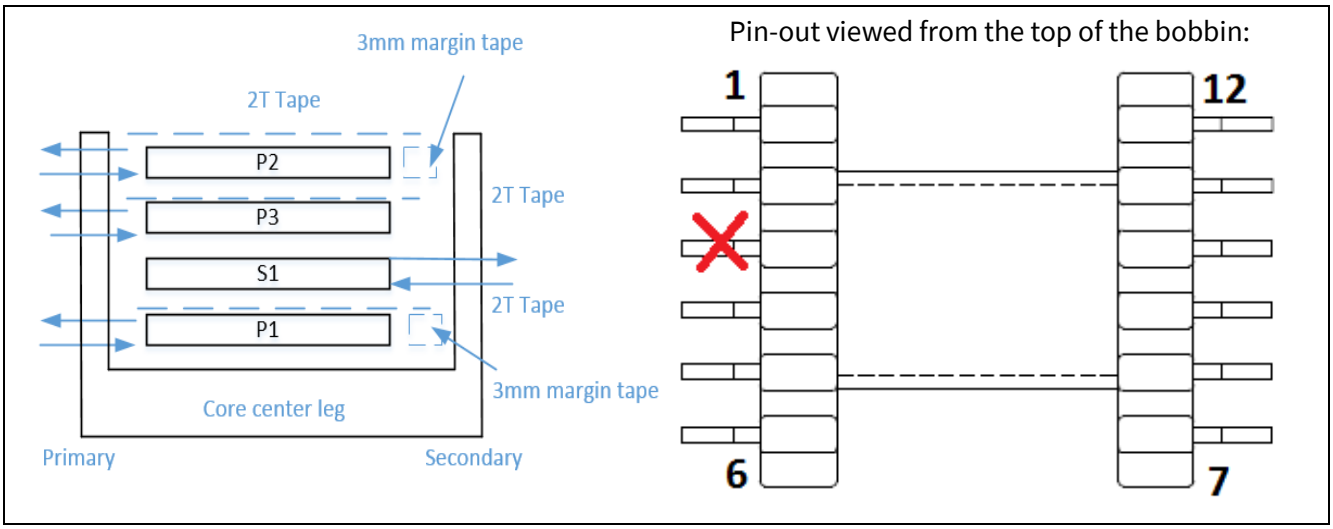

Figure 15 Transformer windings stack-up and pin-out

1. Place 3 mm of margin tape on the secondary side of the transformer (pins 7 to 12).
2. Place two turns of tape over the body of the entire assembly.
3. Place two turns of tape over the bottom of the transformer core or an insulator to provide creepage isolation between the pins and the transformer core.
4. Clip pin 3.

Table 3

Name	Start	Stop	Turns	Wire gauge	Layer	Winding
P1	2	3	65	1 × ϕ 0.15 mm magnet wire	Primary	Evenly spaced
T1			2	Tape to fill window width		
S1	7	8	10	1 × ϕ 0.5 mm triple insulated	12 V_2	Evenly spaced
P3	6	5	10	1 × ϕ 0.5 mm triple insulated	12 V_1	Evenly spaced
T2			2	Tape to fill window width		
P2	3	1	65	1 × ϕ 0.15 mm magnet wire	Primary	Evenly spaced
T3			2	Tape to fill window width		

6 Conclusion

This new bias board was designed to be a replacement for an existing bias module while using the latest devices that are available from Infineon. By switching to the latest available devices and to a snubberless flyback configuration, the efficiency is improved from 10.4 percent to 25 percent over the typical operating load range. The strategies used in this converter, the latest Infineon components, QR operation, removing the snubber network, and an interleaved transformer design can also apply to other low-power bias flyback designs for an overall improvement in performance.

7 References

[1] ICE5QSAG QR Flyback Controller Datasheet

[2] IPU80R4K5P7 800V P7 MOSFET Datasheet

Revision history

Major changes since the last revision

Page or reference	Description of change

Other Trademarks
All referenced product or service names and trademarks are the property of their respective owners.

Edition 2017-11-10

Published by

Infineon Technologies AG

81726 München, Germany

Do you have a question about this document?

Email: erratum@infineon.com

Document reference

AN_201709_PL52_030

IMPORTANT NOTICE

The information given in this document shall in no event be regarded as a guarantee of conditions or characteristics (“Beschaffenheitsgarantie”) .

With respect to any examples, hints or any typical values stated herein and/or any information regarding the application of the product, Infineon Technologies hereby disclaims any and all warranties and liabilities of any kind, including without limitation warranties of non-infringement of intellectual property rights of any third party.

In addition, any information given in this document is subject to customer’s compliance with its obligations stated in this document and any applicable legal requirements, norms and standards concerning customer’s products and any use of the product of Infineon Technologies in customer’s applications.

The data contained in this document is exclusively intended for technically trained staff. It is the responsibility of customer’s technical departments to evaluate the suitability of the product for the intended application and the completeness of the product information given in this document with respect to such application.

For further information on the product, technology, delivery terms and conditions and prices please contact your nearest Infineon Technologies office (**www.infineon.com**).

WARNINGS

Due to technical requirements products may contain dangerous substances. For information on the types in question please contact your nearest Infineon Technologies office.

Except as otherwise explicitly approved by Infineon Technologies in a written document signed by authorized representatives of Infineon Technologies, Infineon Technologies’ products may not be used in any applications where a failure of the product or any consequences of the use thereof can reasonably be expected to result in personal injury.